ACS OMEGA

http://pubs.acs.org/journal/acsodf

Article

Comparison of Serotonin-Regulated Calcific Processes in Aortic and Mitral Valvular Interstitial Cells

Xinmei Wang, Nandini Deb, and Carla M. R. Lacerda*

Cite This: *ACS Omega* 2021, 6, 19494–19505

Read Online

ACCESS | Metrics & More | Article Recommendations

ABSTRACT: Calcification is an important pathological process and a common complication of degenerative valvular heart diseases, with higher incidence in aortic versus mitral valves. Two phenotypes of valvular interstitial cells (VICs), activated VICs and osteoblastic VICs (obVICs), synergistically orchestrate this pathology. It has been demonstrated that serotonin is involved in early stages of myxomatous mitral degeneration, whereas the role of serotonin in calcific aortic valve disease is still unknown. To uncover the link between serotonin and osteogenesis in heart valves, osteogenesis of aortic and mitral VICs was induced in vitro. Actin polymerization and serotonin signaling were inhibited using cytochalasin D and serotonin inhibitors, respectively, to investigate the role of cell activation and serotonin signals in valvular cell osteogenesis. To evaluate calcification progress, calcium and collagen deposits along with the expression of protein markers, including the rate-limiting enzyme of serotonin synthesis [tryptophan hydroxylase 1 (TPH1)], were assessed. When exposed to osteogenic culture conditions and grown on soft surfaces, passage zero aortic VICs increased extracellular collagen deposits and obVIC phenotype markers. A more intense osteogenic process was observed in aortic VICs of higher passages, where cells were activated prior to osteogenic induction. For both, TPH1 expression was upregulated as osteogenesis advanced. However, these osteogenic changes were reversed upon serotonin inhibition. This discovery provides a better understanding of signaling pathways regulating VIC phenotype transformation and explains different manifestations of degenerative pathologies. In addition, the discovery of serotonin-based inhibition of valvular calcification will contribute to the development of potential novel therapies for calcific valvular diseases.

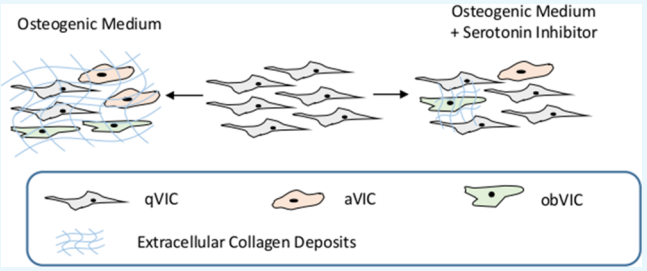

INTRODUCTION

Valvular heart diseases affect approximately 2.8% of the US population, and in 2014, valvular heart disease mortality rates exceeded 25,000.[1,2] Additionally, the prevalence of valvular heart diseases increases sharply with age, and the morbidity of moderate or severe valve disease is as high as 13.3% in the population older than 74 in the US.[3] Among various nonrheumatic acquired valvular diseases, the most commonly occurring ones are aortic valve calcification and myxomatous mitral valve disease.[3] These two valvulopathies are fundamentally different. In calcific aortic valves, calcium deposits form, resulting in valvular stenosis and reduced blood flow.[4] In myxomatous mitral valves, the leaflets are thickened and the annulus is enlarged, which lead to prolapse and/or regurgitation due to imperfect leaflet coaptation.[5] It is yet unclear whether aortic and mitral valves present unique pathological processes due to the valvular architecture or the biomolecular nature of valvular interstitial cells (VICs)[6] or a combination of both.

As the main cell population in heart valves, VICs are the major orchestrators of valvular diseases. Quiescent VICs (qVICs) constitute the main phenotype responsible for maintaining valve homeostasis. qVICs are fibroblastic and have the ability to acquire other phenotypes, which are disease mediators, such as activated VICs (aVICs) or osteoblastic VICs (obVICs).[6] When qVICs acquire myofibroblastic properties, identified by the expression of α-smooth muscle actin (α-SMA, UniProt P62736), they are known to become activated or transformed to aVICs.[6,7] This transformation can be induced by a variety of environmental factors, including standard in vitro culture conditions and cell passaging, and when the aVIC phenotype is abundant, the valvular tissue may show signs of calcific or myxomatous pathologies.[8,9] Myxomatous pathology shows a large population of aVICs and some qVICs, whereas calcific valves show qVICs, aVICs, and a small population of obVICs, which show increased expression of bone markers, including alkaline phosphatase (ALP, UniProt P05196) and osteocalcin (UniProt P02818), indicators of early- and late-stage osteogenesis, respectively, and runt-related transcription factor 2

Received: March 30, 2021
Accepted: June 28, 2021
Published: July 20, 2021

(Runx2, UniProt Q13950) and bone morphogenetic proteins.[10,11] In these valves, aVICs are known to promote dystrophic calcification pathways via apoptotic programs, whereas obVICs are known to promote osteogenic pathways via Wnt and Runx2. Thus, it is likely that in diseased valves and in vitro models using osteogenic media, both dystrophic and ossific modes of calcification occur to some extent.[12,13] This equates to qVICs directly acquiring obVIC phenotypes and qVICs transforming to aVICs and later to obVICs. Both valvular pathologies are associated with extracellular matrix (ECM) remodeling caused by altered levels of matrix metalloproteinases (MMPs) and their inhibitors.[14,15] Distinctions between calcific and myxomatous pathologies are introduced in Table 1.[6,15]

Table 1. Comparison of Degeneration Types in Aortic and Mitral Valves

valve type	degeneration type	transformed VIC phenotype	protein markers	ECM remodeling patterns
aortic	calcification	obVIC and aVIC	ALP	proteoglycan degradation
			osteocalcin	collagen accumulation
			osteopontin	elastic fiber fragmentation
mitral	myxomatous degeneration	aVIC	α-SMA	proteoglycan accumulation
			MMP13	collagen degradation
			SMemb	elastic fiber fragmentation

These unique cell and molecular features of calcific aortic valves and myxomatous mitral valves indicate that specific cell phenotypes are potentially responsible for different valvular disease types, regardless of the differences in the valve architecture.

The effect of serotonin on human heart valves was initially identified from carcinoid syndrome patients or patients treated with fenfluramine/dexfenfluramine.[16] In both cases, there is an increase in peripheral-circulating serotonin. In addition, it has now been established that serotonin can be synthesized by and signal directly in the valvular micro-environment.[17−19] Serotonin cross-talks with the transforming growth factor α1 (TGFβ1, UniProt P01137) signaling pathway, which is involved in myxomatous mitral and calcific aortic degeneration.[20,21] The rate-limiting enzyme for peripheral serotonin synthesis, tryptophan hydroxylase 1 (TPH1, UniProt P17752), is highly expressed in myxomatous mitral valves.[22] Increasing evidence shows that serotonin affects cellular functions mainly via serotonin 2A/B receptor ($5HT_{2A/B}R$, UniProt P28223, P41595), coupled with G protein and activating downstream signaling pathways that mediate pathological changes.[17,23] Moreover, $5HT_{2B}R$ is increased in myxomatous mitral valves when compared to normal valves.[21] In contrast, the serotonin transmembrane transporter (SERT, UniProt P31645) is down-regulated in mitral valve disease,[24] indicating the excess serotonin available for ligand−receptor binding.[25] TPH1 and $5HT_{2B}R$ are co-localized with SMemb[22] and α-SMA[26] in degenerative myxomatous mitral valves, indicating the presence of serotonin in aVICs. In addition, blocking TPH1 or $5HT_{2B}R$ (UniProt P41595) inhibited mechanically triggered myxomatous marker expression in mitral valves.[27] These findings demonstrate that serotonin is locally synthesized by heart valves[27] and is a potential regulator of valvular heart diseases. Serotonin has also been suggested to affect bone biology and regulate bone disorders.[28,29] Such evidence demonstrated that

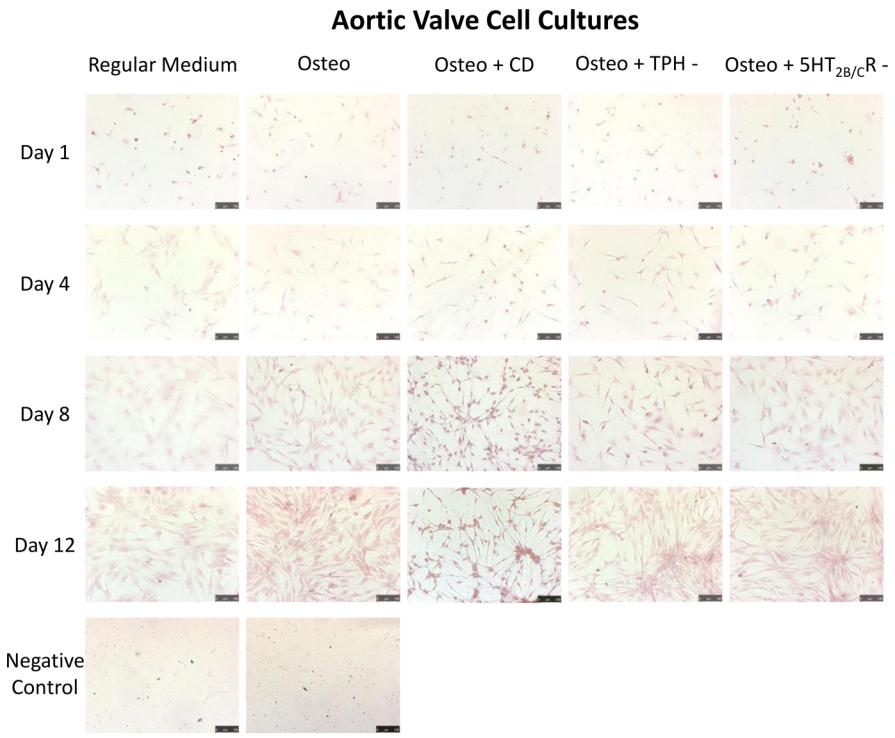

Figure 1. Calcium deposits were detected using alizarin red S in passage zero aortic control and osteogenic cultures, and no positive stains were observed. Osteo: osteogenic medium; osteo + CD: osteogenic medium with CD; osteo + TPH−: osteogenic medium with the TPH inhibitor; and osteo + $5HT_{2B/C}R$: osteogenic medium with the $5HT_{2B/C}R$ inhibitor. Scale bar: 100 μm.

https://doi.org/10.1021/acsomega.1c01723
ACS Omega 2021, 6, 19494−19505

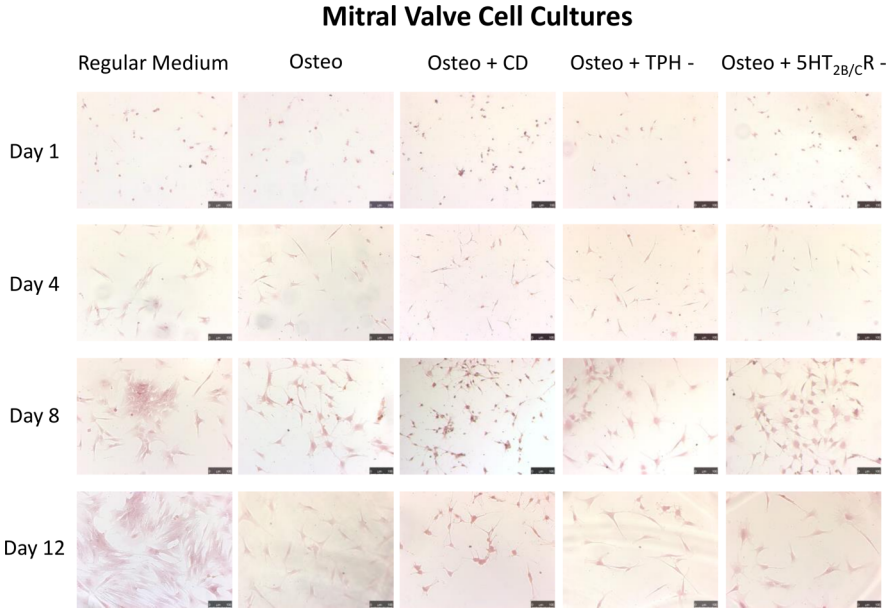

Figure 2. Calcium deposits were detected using alizarin red in passage zero mitral control and osteogenic cultures, and no positive stains were observed. Osteo: osteogenic medium; osteo + CD: osteogenic medium with CD; osteo + TPH−: osteogenic medium with the TPH inhibitor; and osteo + $5HT_{2B/C}R$: osteogenic medium with the $5HT_{2B/C}R$ inhibitor. Scale bar: 100 μm.

peripherally synthesized serotonin inhibits osteogenic bone formation[29,30] via low-density lipoprotein receptor-related protein 5, highly expressed in calcific aortic valves.[11,29] However, the effect of serotonin on bone biology is still heavily debated.[31,32]

Based on current evidence and as introduced above, we hypothesize that there is a link between serotonin and osteogenesis in valvular cells. In this study, we designed an in vitro osteogenic model based on cells freshly harvested from valvular tissues (passage zero) and cultured on soft surfaces. Using this model, we aim to (1) compare the calcification potential of aortic and mitral VICs as assessed by calcium and collagen deposits; (2) investigate phenotype transformation during valvular calcification as indicated by expression of protein markers; and (3) explain the regulatory role of serotonin upon VIC activation or osteoblastic transformation. Results of this study will shed some light on why aortic and mitral valves present unique pathologies when the effect of the valvular architecture is removed. In addition, confirmation of a link between serotonin and osteogenesis will contribute to finding a way to inhibit or slow down calcific pathways in heart valves.

RESULTS AND DISCUSSION

Extracellular Collagen Deposition by Aortic Valve Osteogenic Cultures Was Reversed by Serotonin Inhibitors. Calcium deposits, which commonly serve as a marker of calcification,[13] were analyzed qualitatively using alizarin red S stain. Cell-free and collagen-coated polydimethylsiloxane (PDMS) was stained with alizarin red S as a negative control, and no stains were detected (Figure 1). Up to 12 days in culture, there were no observable calcium deposits in passage zero aortic and mitral cultures under all conditions (Figures 1 and 2). Cytochalasin D (CD) treatment induced the shrinkage of the cell skeleton by blocking the growth of actin filaments,[33] while serotonin inhibitors did not alter cell morphology (Figure 1).

Aniline blue from trichrome stain was used to assess collagen synthesis and secretion, previously reported as a marker of osteogenesis.[34] Similarly, cell-free and collagen-coated PDMS incubated in regular and osteogenic medium was stained in parallel as a negative control, and no fibers were observed (Figure 3A). It appears that the exogenous collagen coating of the wells does not stain positively for collagen, perhaps due to the denaturing conditions of its isolation and preparation in commercial processing. Another possible reason might be that the exogenous collagen coated on the PDMS surface was below the range of minimum detection sensitivity of aniline blue stain or it was positively stained by aniline blue but lower than the visible amount of microscopy observation. Quantitative analysis was performed following an observation of positive collagen stains since day 8 in aortic cultures. In aortic cultures (Figure 3A,B), collagen deposits were significantly increased in osteogenic medium, in line with the observation that cells maintained in osteogenic medium secreted excess collagen starting around day 8, covering the entire culture surface. A similar collagen network was observed in CD-supplemented osteogenic culture. However, it was less pronounced than that from osteogenic culture, potentially due to the alteration in cell morphology. The overproduction of collagen by osteogenic medium was significantly reduced with the presence of serotonin inhibitors (Figure 3B), although these two inhibitors did not exhibit significantly different effects. Moreover, the collagen deposition under the same culture conditions at different time points was not significantly different. The overproduction of collagen fibers was also observed in human calcific aortic valve specimens.[35] Collagen only accumulated in small areas of osteogenic cultures with serotonin inhibitors, even though it seemed that the TPH inhibitor impeded collagen secretion more effectively than the $5HT_{2B/C}R$ inhibitor. These observations indicate that TPH1 and $5HT_{2B/C}R$ inhibitors decreased collagen secretion, in line with another study, which demonstrated that serotonin regulates collagen remodeling in heart valves.[20] Recently, two rodent studies demonstrated the regulatory role of serotonin in valvular calcification at the tissue level[36] and cell

https://doi.org/10.1021/acsomega.1c01723
ACS Omega 2021, 6, 19494−19505

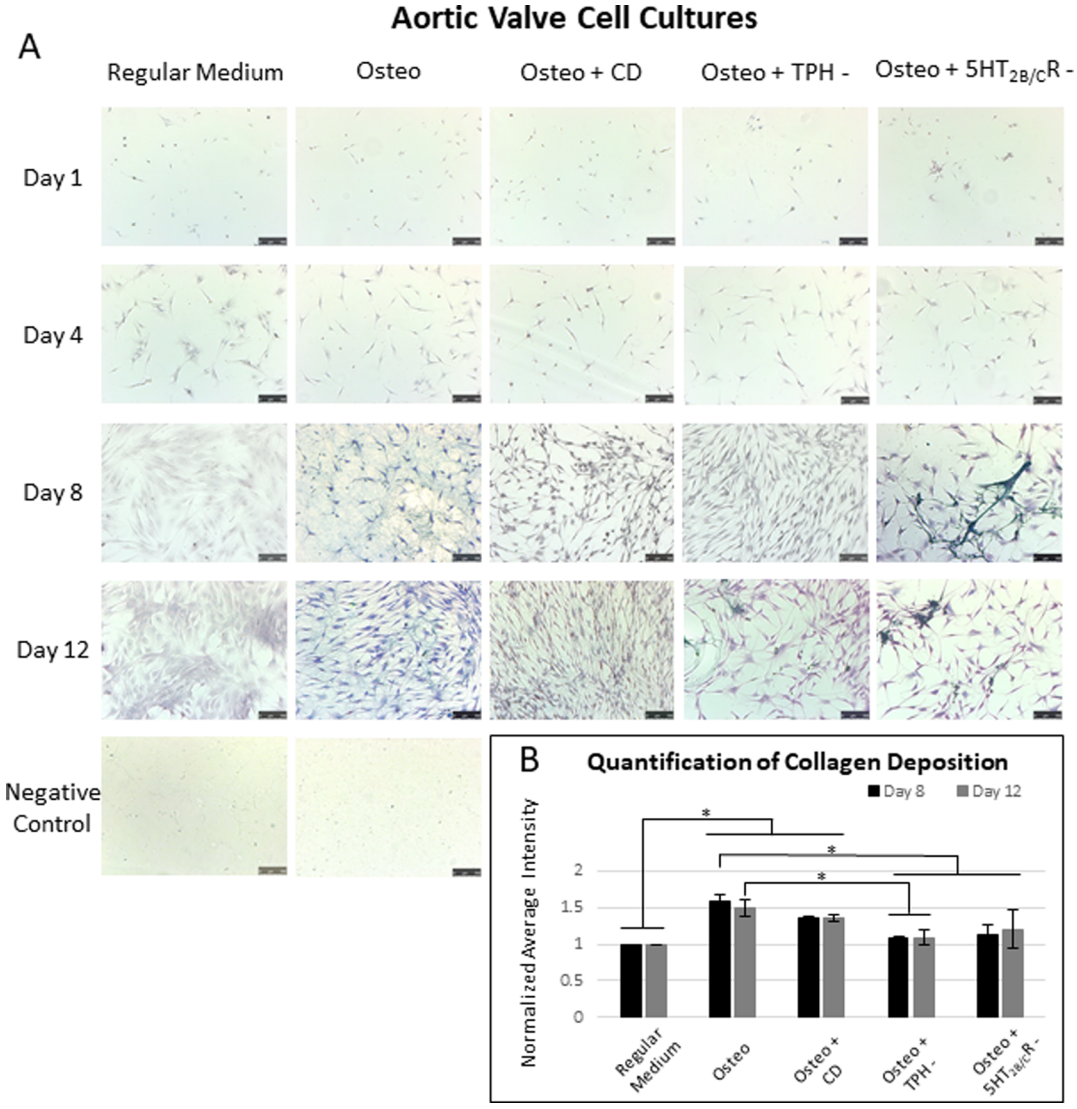

Figure 3. (A) Collagen deposits were detected using aniline blue in passage zero aortic control and osteogenic cultures. Osteogenic medium successfully induced extracellular collagen deposits, as stained in blue. However, this extra collagen production was inhibited by serotonin inhibitors. (B) Collagen deposition in aortic cultures quantified using ImageJ. Osteo: osteogenic medium; osteo + CD: osteogenic medium with CD; osteo + TPH−: osteogenic medium with the TPH inhibitor; and osteo + $5HT_{2B/C}R$: osteogenic medium with the $5HT_{2B/C}R$ inhibitor. Scale bar: 100 μm. The asterisk indicates a significant difference ($p < 0.05$).

level.[37] They suggested that serotonin signaling promotes aortic valve calcification via $5HT_{2B}R$, in line with our mechanistic observation that collagen production and obVIC marker expression were attenuated by the $5HT_{2B/C}R$ inhibitor. Besides, this study strengthens the evidence of serotonin involvement in osteogenic changes of VICs and potential indication that reducing serotonin signaling could slow down the progression of valve cusp calcification. In sharp contrast, no collagen was deposited in control cultures (regular medium) during the entire culture time. In mitral cultures (Figure 4), there was no collagen deposition for over 12 days regardless of medium conditions, indicating a lack of osteogenic or dystrophic calcification. This visible difference in extracellular collagen synthesis between aortic and mitral cell cultures suggested that aortic VICs have a faster and more intense response to osteogenic induction.

Passage Zero Mitral VICs Did Not Adapt to the Osteogenic Environment. Cell viability under osteogenic conditions was monitored for every 4 days up to day 12. Aortic VICs thrived under all medium conditions, as their average viability always remained higher than 96.04% and increased with time (Figure 5A). However, mitral valve interstitial cells maintained a high viability of 96.86 ± 1.54% only in regular medium on day 4, and the viabilities further increased to 99.68 ± 0.37% on day 12 (Figure 5B). Mitral cell viability in osteogenic medium dropped initially to 89.26 ± 5.48% on day 4 without significant change afterward (Figure 5B). In addition, increased loss of viability was observed in inhibitor-supplemented osteogenic cultures, and cell viability tended to further decrease with time, although these differences were not statistically significant (Figure 5B). The lowest mitral cell viability, which is 72.80 ± 10.70%, appeared in the last day of CD-supplemented osteogenic cultures (Figure 5B). One possible explanation for the loss of mitral cells under osteogenic conditions is that, in order to compare with aortic valve cells, they were treated under an oxygen concentration representative of normal arterial blood oxygenation, which is higher than the venous oxygen levels they normally experience in vivo. This may be also caused by the synergistic stress from the osteogenicity-inducing environment

https://doi.org/10.1021/acsomega.1c01723
ACS Omega 2021, 6, 19494−19505

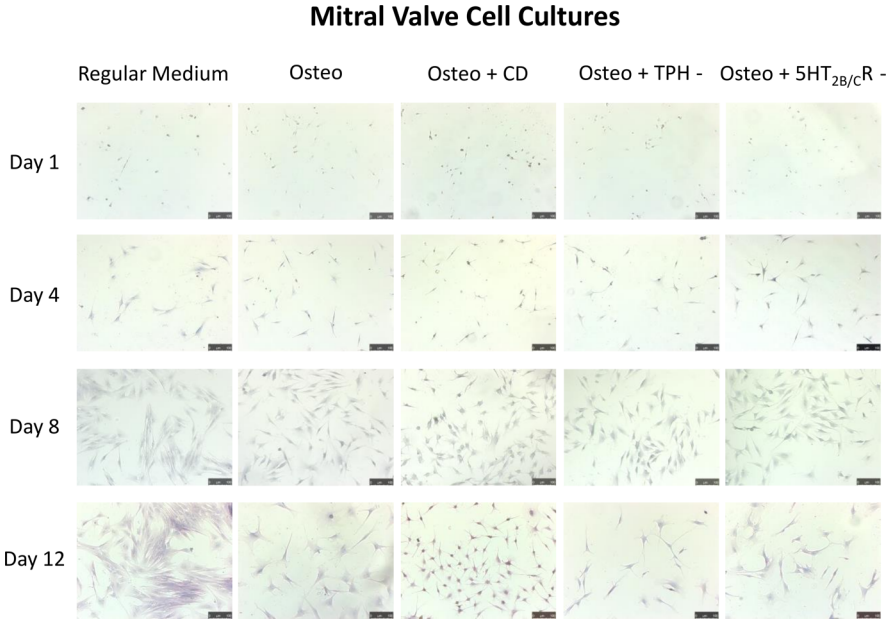

Figure 4. Collagen deposits were detected using aniline blue in passage zero mitral control and osteogenic cultures, and no positive stain was observed. Osteo: osteogenic medium; osteo + CD: osteogenic medium with CD; osteo + TPH−: osteogenic medium with the TPH inhibitor; and osteo + $5HT_{2B/C}R$: osteogenic medium with the $5HT_{2B/C}R$ inhibitor. Scale bar: 100 μm.

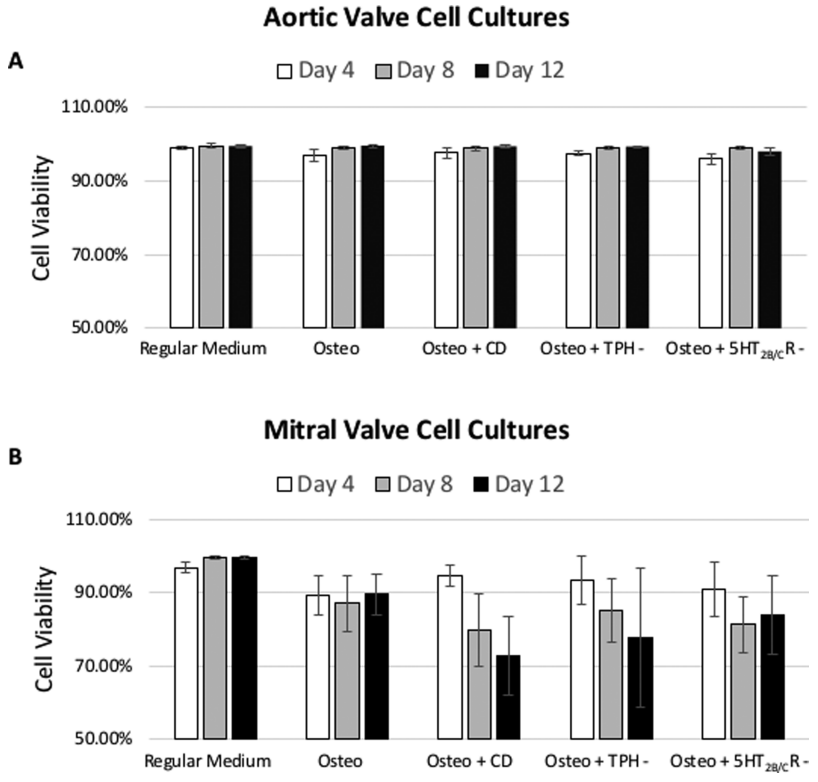

Figure 5. Cell viability of passage zero aortic (A) and mitral (B) control and osteogenic cultures. Osteo: osteogenic medium; osteo + CD: osteogenic medium with CD; osteo + TPH−: osteogenic medium with the TPH inhibitor; and osteo + $5HT_{2B/C}R$: osteogenic medium with the $5HT_{2B/C}R$ inhibitor. Scale bar: 100 μm.

and actin fiber disruption. In line with the reduced cell viability of mitral osteogenic cultures with time, decreased cell density in later cultures was also observed from cellular stain images (Figures 2 and 4). These experiments justify mitral cell loss under different culture conditions, potentially due to cell vulnerability and difficulties in adaptation to osteogenic conditions.

Expression of Osteogenesis Markers by Aortic VICs Was Reversed by Serotonin Inhibitors. According to the abundant collagen deposition (Figure 3) and the absence of calcium deposits (Figure 1) in passage zero aortic valve

https://doi.org/10.1021/acsomega.1c01723
ACS Omega 2021, 6, 19494−19505

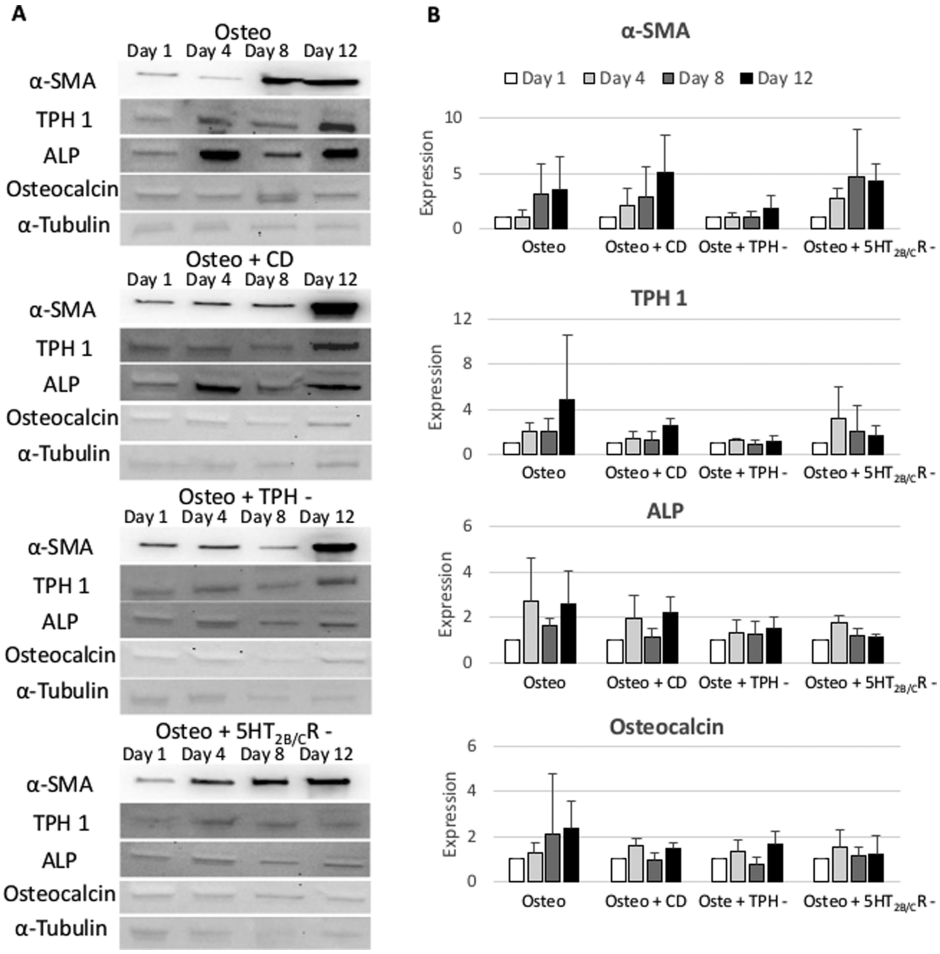

Figure 6. VIC phenotype markers in passage zero aortic osteogenic cultures were evaluated by western blot (A) and quantified (B) using ImageJ. The error bar represents standard deviation from three biological replicates. Osteo: osteogenic medium; osteo + CD: osteogenic medium with CD; osteo + TPH−: osteogenic medium with the TPH inhibitor; and osteo + $5HT_{2B/C}R$: osteogenic medium with the $5HT_{2B/C}R$ inhibitor. Scale bar: 100 μm.

osteogenic cultures, it was determined that osteogenesis was initiated but perhaps not completed. Even though serotonin inhibitors suppressed the synthesis and secretion of collagen, the effect of these inhibitors on VIC phenotype transformation during osteogenesis was still unclear. Thus, the expression levels of aVIC markers (α-SMA and TPH1) and obVIC markers (ALP and osteocalcin) were evaluated by immunoblotting (Figure 6A,B) to determine phenotype transformation during osteogenesis of passage zero aortic VICs and reveal the link between serotonin and valvular cell calcific processes.

Osteogenic Culture. As a marker of aVICs, the expression of α-SMA increased after day 8 (Figure 6B). Along with the increase in α-SMA expression, TPH1, the rate-limiting enzyme of serotonin synthesis, was highly induced only by the last day of culture (Figure 6B). However, before the cell activation as indicated by high expression of α-SMA and TPH1, ALP expression was upregulated on day 4 and remained high until day 12 (Figure 6B). As a marker of the late phase of osteogenesis, osteocalcin expression remained stable across the entire culture time (Figure 6B). Even though these trends were clearly present on bands, they were not significantly different as determined by statistical tests. The same was true for inhibitor-supplemented osteogenic cultures. These observations suggest that passage zero quiescent aortic VICs tend to acquire an osteoblastic phenotype earlier followed by the activated phenotype later in culture, as suggested by a 2.73-fold increase in ALP on day 4 and a 3.11-fold increase in α-SMA on day 8. This discovery is in agreement with the previous observation that activated and obVICs are both functional in mediating valvular calcification.[12,38] Moreover, the presence of obVICs, along with the positive collagen deposition, suggests that aortic cells were undergoing osteogenesis, rather than fibrosis.

Osteogenic Culture with CD. Similarly, the expression of α-SMA (aVIC marker) increased 2.84-fold after day 8; nevertheless, ALP, an osteoblastic phenotype marker, increased 1.95-fold on day 4, prior to cell activation (Figure 6B). It seems that a short CD incubation did not result in any clear changes in protein expression compared to those from osteogenic culture, suggesting that the initiation of valvular cell osteogenesis was not altered by disturbing the polymerization of actin filaments.

Osteogenic Culture with Serotonin Inhibitors. Both the TPH inhibitor and $5HT_{2B/C}R$ inhibitor arrested TPH1 expression in passage zero aortic valve osteogenic culture (Figure 6B). Moreover, α-SMA expression remained unchanged with TPH inhibition by day 8, but $5HTR_{2B/C}R$ seemed to further upregulate α-SMA expression 4.69-fold (Figure 6B). Hence, passage zero aortic VIC activation was linked to the synthesis of serotonin but not linked to its signaling receptor type 2B/C. This might be due to the presence of other functional serotonin receptor subtypes. This could be further explained by intracellular serotonin being needed for α-SMA expression, but its receptor binding, meaning extracellular serotonin, may have a

https://doi.org/10.1021/acsomega.1c01723
ACS Omega 2021, 6, 19494−19505

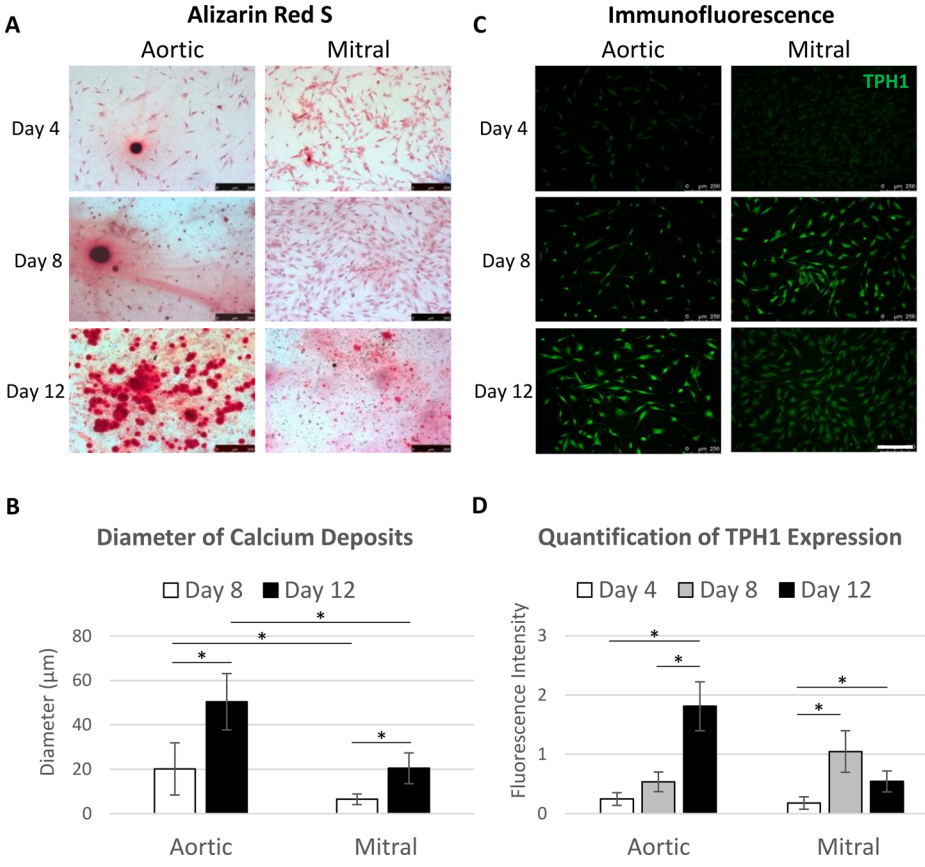

Figure 7. Calcium deposits (A) were detected using alizarin red S and quantified (B) by average aggregate diameters in osteogenic cultures of VICs of higher passages. Immunofluorescent stain of TPH1 (C) and quantification (D) in osteogenic valvular cultures of higher passages. Scale bar: 250 μm. Asterisk indicates a significant difference ($p < 0.05$).

distinct effect. ALP expression increased 2.56-fold in day 12 osteogenic cultures, whereas this upregulation was restrained to 1.54-fold and 1.13-fold by the TPH1 inhibitor and $5HT_{2B/C}R$ inhibitor, respectively (Figure 6B). The suppressive effect of serotonin inhibitors was also observed in another obVIC marker. Osteocalcin expression increased 2.34-fold in day 12 osteogenic cultures, whereas this upregulation was suppressed at 1.64-fold and 1.19-fold by the TPH1 inhibitor and $5HT_{2B/C}R$ inhibitor, respectively (Figure 6B). These two types of serotonin inhibitors both reduced calcific pathways (Figure 6B).

Cell Activation by in Vitro Passaging Strongly Promoted Osteogenesis in Aortic Cultures. In all the results presented above, passage zero VICs were employed due to their physiological quiescent state, as observed on the expression levels of α-SMA. Osteogenic changes were successfully induced by osteogenic medium in passage zero aortic cells, although these osteogenic changes were suppressed by serotonin inhibitors. However, some argue that cell activation is a precondition of osteoblastic transformation in the process of valvular calcification,[39,40] even though this also depends on several factors, such as the interaction with endothelial cells, stiffness of the cell culture substrate, and chemical stimuli.[41,42] Hence, it is valuable and interesting to compare the osteogenesis process of polystyrene plate-activated cells (passage four) and freshly isolated quiescent cells (passage zero) with all other experimental conditions held constant. Previous studies demonstrated that VICs tend to become activated with passaging in vitro in polystyrene dishes.[9,43] A previous study reports that human mesenchymal stem cells have mechanical memory, which affects further differentiation and protein expression.[44] The stiffness-induced VIC activation is expected to be maintained after transfer to the PDMS surface, although VICs may have less memory than stem cells. VICs of passage 4–5 were transferred from polystyrene dishes to collagen-coated PDMS and maintained in osteogenic medium for 12 days. As before, calcium deposits were detected for every 4 days in cells of higher passages. As presented in Figure 7A, calcium deposits were observed in both aortic and mitral VICs of higher passages starting on day 4, and this increased with time. However, at any given time point, the abundance of calcium precipitates was larger in aortic than in mitral cultures (Figure 7A). In day 12 aortic cultures, calcium deposits distributed across the entire monolayer surface, which is consistent with observations from human calcific aortic valve specimens.[11] The diameters of calcium precipitates were quantified and compared between paired time points and valve types (Figure 7B). From day 8 to day 12, the diameter of calcium precipitates increased from 20.15 ± 11.78 to 50.40 ± 12.65 μm in aortic cultures, while the diameter of calcium precipitates increased from 6.47 ± 2.40 to 20.44 ± 6.91 μm in mitral cultures. Despite the larger increase in aortic cultures, the size of calcium precipitates significantly increased in the last 4 days in both valve cultures (Figure 7B). At the same time point, calcium precipitates produced by aortic valve cells were significantly larger than those from mitral valve cell cultures (Figure 7B). To the best of our knowledge, there was only one study presenting calcium precipitation by mitral valve cells previously,[45] and its observation was consistent with ours in that mitral VICs secreted and precipitated less calcium

https://doi.org/10.1021/acsomega.1c01723
ACS Omega 2021, 6, 19494−19505

than aortic VICs. Calcium deposition was extremely increased in aortic VICs of higher passages rather than passage zero, indicating that cell activation promoted or at least accelerated valvular cell osteogenesis.

The involvement of serotonin in valvular cell osteogenesis was validated in cells of higher passages by immunofluorescence, as shown in Figure 7C,D. In aortic cultures, the expression of TPH1 slightly increased from day 4 to day 8, as suggested by the fluorescence intensity increase from 0.25 ± 0.11 to 0.53 ± 0.17. However, the fluorescence intensity on day 12 was largely increased to 1.81 ± 0.41, indicating a significant upregulation of TPH1 expression in the following 4 days (Figure 7D). This finding agrees with the increase in TPH1 expression with time from passage zero aortic osteogenic cultures (Figure 6B). In mitral cultures, expression of TPH1 was extremely low (fluorescence intensity of 0.17 ± 0.10) on day 4 but significantly increased on day 8 (fluorescence intensity of 1.05 ± 0.35) followed by a drop on day 12 (fluorescence intensity of 0.54 ± 0.18) (Figure 7D). These differences could explain why calcification is the most commonly observed degenerative phenotype in aortic valves but not in mitral valves. Different behaviors of aortic and mitral VICs under osteogenic conditions probably relate to in vivo cartilage development in mitral valves[46] compared to bone formation in aortic valves.[11,47]

Final Remarks and Limitations. Thus far, the knowledge of signaling pathways mediating VIC phenotype transformation in degenerative valvular disease is limited.[48] A cell culture model was used in this work to provide a better understanding of the responses of mitral and aortic VICs to osteogenic conditions. More importantly, we further confirmed the link between serotonin and osteogenesis in valvular cells, according to the observation that serotonin inhibitors suppressed medium-induced osteogenesis. In aortic cultures, lower serotonin resulted in reduced transformation to the osteoblastic phenotype, which conflicts with previous results of bone formation.[49] There may be several potential explanations. First, the inducer effect of serotonin on bone formation was discovered in a mouse model, which might be a net consequence of interactions with a multitude of other signaling pathways. On the other hand, an in vitro study demonstrated that serotonin could be induced by mechanical stimuli and locally synthesized in heart valves.[50] Similarly, this study focused on valvular cells and specifically on the effect of locally synthesized serotonin on valvular cell osteogenesis in a simplified in vitro system without the influence of surrounding tissues. Second, it has been proposed that the effect of serotonin on bone formation is dose-dependent,[51] which may make the correlation between serotonin and osteogenesis vary with the ratio of serotonin concentration and cell density. Hence, the difference in serotonin action on the heart valves and bone might be due to the large disparity in concentrations of serotonin synthesized by the heart valves and gut.[49,50]

There are limitations in this study. First, porcine VICs were employed in this study, and they could not represent the same physiological structure and function of human VICs.[52] Despite this limitation being common to animal models, porcine is still reliable and widely used in studies of human heart disease, particularly those of heart valvular degeneration.[53−55] Second, the disruption of actin fiber polymerization did not affect osteogenic-induced calcification in VICs, potentially due to the limited incubation time with CD, although a similar finding was stated in previous work.[39] Third, culture medium was replaced for every 3 days, which may cause loss of calcium deposits and impact the trends of protein expression due to altered metabolic rate. Despite these experimental limitations, this study revealed the major novel finding that inhibition of serotonin synthesis highly attenuated VIC phenotype transformation and extracellular collagen precipitation induced by osteogenic medium. In addition, cell activation induced by cell passaging in vitro promoted osteogenesis in aortic VICs with abundant calcium deposits and significantly increased TPH1 expression. In this case, serotonin may be a potential target to prevent or slow down valvular calcific pathways.

■ CONCLUSIONS

The pathological process of calcification of aortic and mitral VICs was studied in an in vitro porcine model. A mild osteogenic process was initiated in passage zero aortic rather than mitral VIC cultures by osteogenic medium, as indicated by increased extracellular collagen deposits and expression of obVIC and aVIC markers. A complete osteogenic process was observed in aortic and mitral VICs of higher passages, where cells were activated prior to osteogenic induction. In both cases, TPH1 expression was upregulated with the progress of aortic VIC osteogenesis. However, all of these effects were decreased upon serotonin inhibition in aortic VIC osteogenic cultures. This discovery provides insights into the regulation of VIC phenotype transformation and suggests that aortic cells have a higher potential for calcification than mitral cells, regardless of the valvular architecture. In addition, the discovery of serotonin-based inhibition of valvular calcification pathways will contribute to the development of potential novel therapies for calcific valvular diseases.

■ MATERIALS AND METHODS

Cell Isolation and Culture Preparation. Whole aortic and mitral valves were harvested from fresh porcine hearts obtained from a local abattoir following previously established protocols.[56] Once aortic and mitral valves were obtained, they were washed in sterile phosphate-buffered saline [PBS, 137 mM sodium chloride, 4.3 mM sodium phosphate dibasic, 2.7 mM potassium chloride, and 1.46 mM potassium phosphate monobasic (all from Fisher Scientific, Waltham, MA)] with 2% penicillin/streptomycin/amphotericin b (MP Biomedicals, Santa Ana, CA) at least three times. First, valvular endothelial cells from both surfaces were removed using a sterile soft brush after 10 min of incubation in 600 U/mL collagenase (Sigma-Aldrich, St. Louis, MO) solution, which was prepared in fresh culture medium [89% Dulbecco's modified Eagle medium (Mediatech, Corning, Manassas, VA), 10% fetal bovine serum (Atlanta Biologicals, Flowery Branch, GA), 1% penicillin/streptomycin/amphotericin b], at 37 °C in a humidified atmosphere and 5% CO_2. Similarly, endothelium-free valves underwent overnight collagenase (UniProt P03956) digestion for VIC isolation. Subsequently, passage zero VICs were directly cultured in regular or osteogenic medium in the presence or absence of inhibitors at 37 °C in a humidified atmosphere and 5% CO_2 for initial acclimation.[9] In parallel, VICs were also maintained on plastic surfaces in regular medium until passage 4−5 for higher passage studies.

Osteogenic Cultures on Soft Substrates. Unlike many studies of VIC osteogenesis, which employed potentially transformed VICs in culture, our model utilized passage zero cells in comparison to higher passages and soft culture surfaces. To improve adhesion, PDMS membranes of 0.5 mm thickness

https://doi.org/10.1021/acsomega.1c01723
ACS Omega 2021, 6, 19494−19505

(Rogers Corporation, Chandler, AZ) were autoclaved for 20 min and incubated with 200 μg/mL collagen (UniProt P02452) solution (Advanced Biomatrix, Carlsbad, CA) in sterile PBS at 37 °C overnight. After collagen coating, PDMS membranes were washed with sterile PBS prior to cell seeding. Young's modulus of PDMS used for cell culture was 0.49 ± 0.02 MPa, obtained from dynamic mechanical analysis experiments. This value falls between Young's modulus of the first and second linear elastic phase of aortic valves estimated by others.[57] After collagen coating of PDMS, the water contact angle increased from 6 to 98° on average, providing hydrophilic conditions and binding sites for cell attachment and proliferation.

Both porcine aortic VICs and porcine mitral VICs were seeded at a density of 1.1×10^4 cells/cm^2 on collagen-coated PDMS. Cells were maintained for 12 days in regular medium, serving as control, and osteogenic medium (osteo) (LM-0023, OsteoLife Biomedical, Miami, FL) containing 1% penicillin/streptomycin/amphotericin b. Osteogenic cultures were further treated as described below.

Inhibition of Actin Fiber Formation. CD is a well-known inhibitor of actin filament polymerization,[33] which in principle leads to inhibition of VIC activation. CD (Sigma-Aldrich) stock solution of 1 mg/mL was prepared in dimethyl sulfoxide (DMSO) (Fisher Scientific).[58] Cells were cultured in osteogenic medium supplemented with 1 μg/mL CD (osteo + CD) for 1 h prior to calcification assessment on days 1, 4, 8, and 12. A DMSO control culture was prepared by culturing cells in osteogenic medium containing 0.1% DMSO (v/v), and no effect on cells was observed, as suggested by a previous study.[58]

Serotonin Inhibition. As introduced above, serotonin synthesis is regulated using TPH1, and after its secretion, the receptor $5HT_{2B}R$ plays a role in initiating extracellular signaling.[17] To uncover the role of serotonin in valvular calcific processes, inhibition of serotonin signaling was achieved in two ways, as described previously.[27] Serotonin synthesis was inhibited using 250 μM 4-chloro-DL-phenylalanine (Sigma-Aldrich), an inhibitor of TPH. Serotonin receptors, 2B/2C ($5HT_{2B/C}R$), were blocked using 10 μM SB-206553 hydrochloride hydrate (Sigma-Aldrich). Cells were continually incubated in osteogenic medium with serotonin inhibitors (osteo + TPH− or osteo + $5HT_{2B/C}R$−) for 12 days, with medium replacement every other day. Calcium and collagen accumulation along with the expression of protein markers was investigated on days 1, 4, 8, and 12.

Cell Viability Assay. Cell viability from all control and osteogenic cultures was assessed using the ReadyProbes cell viability imaging kit (Thermo Fisher Scientific, Waltham, MA) on days 4, 8, and 12. As suggested by the protocol from the manufacturer, two drops of each stain were added to every milliliter of medium and incubated with cells at 37 °C for 20 min. As a consequence, nuclei of live and dead cells were labeled using a live reagent (Hoechst 33342) and dead reagent and visualized in blue and green, respectively, under fluorescent microscopy. Fluorescent images were acquired using a fluorescent camera (DFC365 FX) of the Leica AF6000 microsystem (Leica Microsystems, Buffalo Grove, IL). The number of live cells and dead cells from each fluorescent image was counted using MATLAB R2018b (MathWorks, Natick, MA). Cell viability was calculated by the number of live cells over the number of total cells. Average cell viability of each time point and medium condition was determined from at least nine technical replicates of 10× fluorescent images (three biological replicates), and cell density varied around 800 cells/image depending on the time point and medium conditions. Their statistically significant differences were assessed by Kruskal−Wallis and multiple comparison tests. $p < 0.05$ was considered significant.

Immunofluorescence. Cells were fixed in 2% formaldehyde solution (Fisher Scientific) for 10 min, followed by permeabilization with 0.1% Igepal (Sigma-Aldrich) for 5 min. Nonspecific binding was blocked with 1% goat serum (MP Biomedicals) for 30 min. The primary antibody used was mouse monoclonal anti-TPH (EMD Millipore, Temecula, CA) at a final concentration of 1 μg/mL. After 1.5 h of incubation with primary antibodies, cells were incubated in the dark with the DyLight 488-conjugated goat anti-mouse IgG secondary antibody (Fisher Scientific) at a final concentration of 0.5 μg/mL for 1.5 h. Then, the actin cytoskeleton and nuclei were counterstained with 0.5 U/mL rhodamine phalloidin stain for 30 min and 1 μg/mL 4′,6-diamidino-2-phenylindole stain (Molecular Probes, Eugene, OR) for 1 min. TPH1, actin filaments, and nuclei were visualized in green, yellow, and blue under the corresponding excitation and emission wavelengths. For each treatment, over 50 fluorescent images were acquired using a fluorescent camera (DFC365 FX) of the Leica AF6000 microsystem. Relative fluorescence intensities of TPH1 were quantified using ImageJ (image processing and analysis in Java by NIH Image, National Institute of Health, Bethesda, MD), and their statistically significant differences were assessed by Kruskal−Wallis and multiple comparison tests. $p < 0.05$ was considered significant.

Assessment of Calcification Endpoints. *Mineralization Assay.* Calcium deposition was assessed for every 4 days in control and all osteogenic treatments. Cells were fixed in 2% formaldehyde solution for 30 min, followed by PBS wash, and stained with 2% alizarin red S (Sigma-Aldrich, pH = 4.2) for 50 min at room temperature. Extracellular calcium precipitates were stained red. Bright-field images were acquired using a color camera. Average diameters of calcium nodules were determined from at least 10 measurements in IrfanView (version 4.38, developed by Irfan Skiljan). With the expectation of observing extracellular calcium deposition, we believe that bright-field images, which clearly present calcium deposit size and distribution, give a more complete picture than simple alizarin red absorbance. Statistically significant differences in diameters of calcium between two time points of the same cell population (aortic or mitral) or two cell populations at the same time point were assessed by the Friedman test and Mann−Whitney *U*-test, respectively, and $p < 0.05$ was considered significant.

Trichrome Stain. Collagen fibers formed in osteogenic cultures were visualized using Gomori's trichrome stain.[59] A Gomori trichrome kit (Fisher Scientific) was used, and the standard staining protocol was followed. Briefly, after fixation, nuclei were labeled using Weigert's iron hematoxylin in dark purple, followed by collagen being stained with aniline blue in blue. Color images from positive-collagen stain areas were acquired as mentioned above. Collagen deposition was quantified by measuring the average gray values using ImageJ. These intensities of cytochemical stains were normalized by the intensity of regular medium at the corresponding time point. Statistically significant differences were assessed by Kruskal−Wallis and multiple comparison tests. $p < 0.05$ was considered significant.

Immunoblotting. Aortic valve cells from each treatment were lysed at 4 °C in protein extraction buffer containing 150 mM sodium chloride and 50 mM *N*-(2-hydroxyethyl)-piperazine-*N*′-ethanesulfonic acid buffer (pH = 7.4) supple-

https://doi.org/10.1021/acsomega.1c01723
ACS Omega 2021, 6, 19494−19505

mented with 2 mM dithiothreitol (DTT) (Fisher Scientific), 25 μg/mL digitonin (Sigma-Aldrich), 1% Igepal (Sigma-Aldrich), and 1% protease inhibitor cocktail (Active Motif, Carlsbad, CA) for 1−2 h. The concentration of each protein sample was determined by bicinchoninic acid protein assay (Fisher Scientific). After quantification, 25 μg of protein load from each treatment was precipitated in nine volumes of ethanol at −80 °C overnight. After precipitation, proteins were redissolved and boiled in Laemmli buffer containing 1 mM DTT. Proteins were separated using 1D gel electrophoresis and transferred to polyvinylidene difluoride membranes. Subsequently, membranes were washed in water, followed by incubation with primary antibodies overnight at 4 °C. The primary antibodies used were mouse monoclonal anti-smooth muscle actin at a final concentration of 1 μg/mL (Fisher Scientific), mouse monoclonal anti-TPH at a final concentration of 1 μg/mL, mouse monoclonal anti-ALP (Santa Cruz Biotechnology, Dallas, TX) at a final concentration of 0.4 μg/mL, mouse monoclonal anti-osteocalcin (Fisher Scientific) at a final concentration of 0.57 μg/mL, and mouse monoclonal anti-α-tubulin (α-tubulin) at a final concentration of 1 μg/mL (Fisher Scientific) that serves as a loading control. All primary antibodies were prepared in tris-buffered saline (TBS, 1×) [10 mM Tris base, 150 mM sodium chloride (both from Fisher Scientific), pH = 8.0] with 5% nonfat milk. Horseradish peroxidase-conjugated secondary antibodies, anti-mouse (Anaspec, Fremont, CA) or anti-rabbit (Anaspec), were diluted in TBS to 1 μg/mL and added for 1 h incubation. After four washes in TBS and ultrapure water, proteins were detected by enhanced chemiluminescence (Bio-Rad, Hercules, CA) with 1:1 mixture of luminol and peroxide solution. Images were acquired using the ChemiDoc imaging system (Bio-Rad) and quantified using ImageJ (n = 3) based on protein band intensity, and bands from day 4, 8, and 12 were normalized by the intensity of the corresponding α-tubulin and day 1 bands. Their statistically significant differences were assessed by Kruskal−Wallis and multiple comparison tests. $p < 0.05$ was considered significant.

■ ASSOCIATED CONTENT

Accession Codes

α-SMA: P62736, $5HT_{2A}R$: P28223, ALP: P05196, $5HT_{2B}R$: P41595, osteocalcin: P02818, SERT: P31645, TGFβ1: P01137, collagenase: P03956, TPH1: P17752, and collagen: P02452.

■ AUTHOR INFORMATION

Corresponding Author

Carla M. R. Lacerda − *Department of Chemical Engineering, Texas Tech University, Lubbock, Texas 79409-3121, United States*; Phone: 806-834-4089; Email: carla.lacerda@ttu.edu; Fax: 806-742-3552

Authors

Xinmei Wang − *Department of Bioengineering, Shenyang University, Shenyang, Liaoning 110044, China*; orcid.org/0000-0003-0604-5579

Nandini Deb − *Department of Chemical Engineering, Texas Tech University, Lubbock, Texas 79409-3121, United States*

Complete contact information is available at: https://pubs.acs.org/10.1021/acsomega.1c01723

Author Contributions

X.W.: conceptualization and design, investigation, data collection, data analysis and interpretation, and manuscript writing; N.D.: data collection and data analysis and interpretation; and C.M.R.L.: conceptualization and design, financial support, data analysis and interpretation, manuscript review and editing, final approval of the manuscript, and project administration.

Notes

The authors declare no competing financial interest.

■ ACKNOWLEDGMENTS

The authors acknowledge Texas Tech University for providing startup funds to C.M.R.L. to support this study. The authors thank Jackson Brothers Meat Locker for providing porcine hearts.

■ REFERENCES

(1) Coffey, S.; Cox, B.; Williams, M. J. A. Lack of Progress in Valvular Heart Disease in the Pre-Transcatheter Aortic Valve Replacement Era: Increasing Deaths and Minimal Change in Mortality Rate over the Past Three Decades. *Am. Heart J.* **2014**, *167*, 562−567.e2.

(2) Benjamin, E. J.; Virani, S. S.; Callaway, C. W.; Chamberlain, A. M.; Chang, A. R.; Cheng, S.; Chiuve, S. E.; Cushman, M.; Delling, F. N.; Deo, R.; de Ferranti, S. D.; Ferguson, J. F.; Fornage, M.; Gillespie, C.; Isasi, C. R.; Jiménez, M. C.; Jordan, L. C.; Judd, S. E.; Lackland, D.; Lichtman, J. H.; Lisabeth, L.; Liu, S.; Longenecker, C. T.; Lutsey, P. L.; Mackey, J. S.; Matchar, D. B.; Matsushita, K.; Mussolino, M. E.; Nasir, K.; O'Flaherty, M.; Palaniappan, L. P.; Pandey, A.; Pandey, D. K.; Reeves, M. J.; Ritchey, M. D.; Rodriguez, C. J.; Roth, G. A.; Rosamond, W. D.; Sampson, U. K. A.; Satou, G. M.; Shah, S. H.; Spartano, N. L.; Tirschwell, D. L.; Tsao, C. W.; Voeks, J. H.; Willey, J. Z.; Wilkins, J. T.; Wu, J. H.; Alger, H. M.; Wong, S. S.; Muntner, P. Heart Disease and Stroke Statistics—2018 Update: A Report From the American Heart Association. *Circulation* **2018**, *137*, e67−e492.

(3) Nkomo, V. T.; Gardin, J. M.; Skelton, T. N.; Gottdiener, J. S.; Scott, C. G.; Enriquez-Sarano, M. Burden of Valvular Heart Diseases: A Population-Based Study. *Lancet* **2006**, *368*, 1005−1011.

(4) Rajamannan, N. M.; Evans, F. J.; Aikawa, E.; Grande-Allen, K. J.; Demer, L. L.; Heistad, D. D.; Simmons, C. A.; Masters, K. S.; Mathieu, P.; O'Brien, K. D.; Schoen, F. J.; Towler, D. A.; Yoganathan, A. P.; Otto, C. M. Calcific Aortic Valve Disease: Not Simply a Degenerative Process: A Review and Agenda for Research from the National Heart and Lung and Blood Institute Aortic Stenosis Working Group. *Circulation* **2011**, *124*, 1783−1791.

(5) Fox, P. R. Pathology of Myxomatous Mitral Valve Disease in the Dog. *J. Vet. Cardiol.* **2012**, *14*, 103−126.

(6) Liu, A. C.; Joag, V. R.; Gotlieb, A. I. The Emerging Role of Valve Interstitial Cell Phenotypes in Regulating Heart Valve Pathobiology. *Am. J. Pathol.* **2007**, *171*, 1407−1418.

(7) Rabkin, E.; Aikawa, M.; Stone, J. R.; Fukumoto, Y.; Libby, P.; Schoen, F. J. Activated Interstitial Myofibroblasts Express Catabolic Enzymes and Mediate Matrix Remodeling in Myxomatous Heart Valves. *Circulation* **2001**, *104*, 2525−2532.

(8) Horne, T.; VandeKopple, M.; Sauls, K.; Koenig, S.; Anstine, L.; Garg, V.; Norris, R.; Lincoln, J. Dynamic Heterogeneity of the Heart Valve Interstitial Cell Population in Mitral Valve Health and Disease. *J. Cardiovasc. Dev. Dis.* **2015**, *2*, 214−232.

(9) Ali, M. S.; Deb, N.; Wang, X.; Rahman, M.; Christopher, G. F.; Lacerda, C. M. R. Correlation between Valvular Interstitial Cell Morphology and Phenotypes: A Novel Way to Detect Activation. *Tissue Cell* **2018**, *54*, 38−46.

(10) Masjedi, S.; Amarnath, A.; Baily, K. M.; Ferdous, Z. Comparison of Calcification Potential of Valvular Interstitial Cells Isolated from Individual Aortic Valve Cusps. *Cardiovasc. Pathol.* **2016**, *25*, 185−194.

(11) Caira, F. C.; Stock, S. R.; Gleason, T. G.; McGee, E. C.; Huang, J.; Bonow, R. O.; Spelsberg, T. C.; McCarthy, P. M.; Rahimtoola, S. H.; Rajamannan, N. M. Human Degenerative Valve Disease Is Associated With Up-Regulation of Low-Density Lipoprotein Receptor-Related

Protein 5 Receptor-Mediated Bone Formation. *J. Am. Coll. Cardiol.* **2006**, *47*, 1707−1712.
(12) Bowler, M. A.; Merryman, W. D. In Vitro Models of Aortic Valve Calci Fi Cation: Solidifying a System. *Cardiovasc. Pathol.* **2015**, *24*, 1−10.
(13) Merryman, W. D.; Schoen, F. J. Mechanisms of Calcification in Aortic Valve Disease: Role of Mechanokinetics and Mechanodynamics. *Curr. Cardiol. Rep.* **2013**, *15*, 355.
(14) Aupperle, H.; März, I.; Thielebein, J.; Kiefer, B.; Kappe, A.; Schoon, H.-A. Immunohistochemical Characterization of the Extracellular Matrix in Normal Mitral Valves and in Chronic Valve Disease (Endocardiosis) in Dogs. *Res. Vet. Sci.* **2009**, *87*, 277−283.
(15) Hinton, R. B.; Yutzey, K. E. Heart Valve Structure and Function in Development and Disease. *Annu. Rev. Physiol.* **2011**, *73*, 29−46.
(16) Surapaneni, P.; Vinales, K. L.; Najib, M. Q.; Chaliki, H. P. Valvular Heart Disease with the Use of Fenfluramine-Phentermine. *Tex. Heart Inst. J.* **2011**, *38*, 581−583.
(17) Hutcheson, J. D.; Setola, V.; Roth, B. L.; Merryman, W. D. Serotonin Receptors and Heart Valve Disease-It Was Meant 2B. *Pharmacol. Ther.* **2011**, *132*, 146−157.
(18) Oyama, M. A.; Levy, R. J. Insights into Serotonin Signal Ing Mechanisms Associated with Canine Degenerative Mitral Valve Disease. *J. Vet. Intern. Med.* **2010**, *24*, 27−36.
(19) Goldberg, E.; Grau, J. B.; Fortier, J. H.; Salvati, E.; Levy, R. J.; Ferrari, G. Serotonin and Catecholamines in the Development and Progression of Heart Valve Diseases. *Cardiovasc. Res.* **2017**, *113*, 849−857.
(20) Jian, B.; Xu, J.; Connolly, J.; Savani, R. C.; Narula, N.; Liang, B.; Levy, R. J. Serotonin Mechanisms in Heart Valve Disease I: Serotonin-Induced up-Regulation of Transforming Growth Factor-Beta1 via G-Protein Signal Transduction in Aortic Valve Interstitial Cells. *Am. J. Pathol.* **2002**, *161*, 2111−2121.
(21) Disatian, S.; Orton, E. C. Autocrine Serotonin and Transforming Growth Factor Beta 1 Signaling Mediates Spontaneous Myxomatous Mitral Valve Disease. *J. Heart Valve Dis.* **2009**, *18*, 44−51.
(22) Disatian, S.; Lacerda, C. M. R.; Orton, E. C. Tryptophan Hydroxylase 1 Expression Is Increased in Phenotype-Altered Canine and Human Degenerative Myxomatous Mitral Valves. *J. Heart Valve Dis.* **2010**, *19*, 71−78.
(23) Xu, J.; Jian, B.; Chu, R.; Lu, Z.; Li, Q.; Dunlop, J.; Rosenzweig-Lipson, S.; McGonigle, P.; Levy, R. J.; Liang, B. Serotonin Mechanisms in Heart Valve Disease II: The 5-HT2 Receptor and Its Signaling Pathway in Aortic Valve Interstitial Cells. *Am. J. Pathol.* **2002**, *161*, 2209−2218.
(24) Scruggs, S. M.; Disatian, S.; Orton, E. C. Serotonin Transmembrane Transporter Is Down-Regulated in Late-Stage Canine Degenerative Mitral Valve Disease. *J. Vet. Cardiol.* **2010**, *12*, 163−169.
(25) Ni, W.; Watts, S. W. 5-Hydroxytryptamine in the Cardiovascular System: Focus on the Serotonin Transporter (SERT). *Clin. Exp. Pharmacol. Physiol.* **2006**, *33*, 575−583.
(26) Cremer, S. E.; Zois, N. E.; Moesgaard, S. G.; Ravn, N.; Cirera, S.; Honge, J. L.; Smerup, M. H.; Hasenkam, J. M.; Sloth, E.; Leifsson, P. S.; Falk, T.; Oyama, M. A.; Orton, C.; Martinussen, T.; Olsen, L. H. Serotonin Markers Show Altered Transcription Levels in an Experimental Pig Model of Mitral Regurgitation. *Vet. J.* **2015**, *203*, 192−198.
(27) Lacerda, C. M. R.; Kisiday, J.; Johnson, B.; Orton, E. C. Local Serotonin Mediates Cyclic Strain-Induced Phenotype Transformation, Matrix Degradation, and Glycosaminoglycan Synthesis in Cultured Sheep Mitral Valves. *Am. J. Physiol.: Heart Circ. Physiol.* **2012**, *302*, H1983−H1990.
(28) Yadav, V. K.; Ducy, P. Lrp5 and Bone Formation: A Serotonin-Dependent Pathway. *Ann. N.Y. Acad. Sci.* **2010**, *1192*, 103−109.
(29) Ducy, P.; Karsenty, G. The Two Faces of Serotonin in Bone Biology. *J. Cell Biol.* **2010**, *191*, 7−13.
(30) Ducy, P. 5-HT and Bone Biology. *Curr. Opin. Pharmacol.* **2011**, *11*, 34−38.
(31) Cui, Y.; Niziolek, P. J.; MacDonald, B. T.; Zylstra, C. R.; Alenina, N.; Robinson, D. R.; Zhong, Z.; Matthes, S.; Jacobsen, C. M.; Conlon, R. A.; Brommage, R.; Liu, Q.; Mseeh, F.; Powell, D. R.; Yang, Q. M.; Zambrowicz, B.; Gerrits, H.; Gossen, J. A.; He, X.; Bader, M.; Williams, B. O.; Warman, M. L.; Robling, A. G. Lrp5 Functions in Bone to Regulate Bone Mass. *Nat. Med.* **2011**, *17*, 684−691.
(32) Cui, Y.; Niziolek, P. J.; MacDonald, B. T.; Alenina, N.; Matthes, S.; Jacobsen, C. M.; Conlon, R. A.; Brommage, R.; Powell, D. R.; He, X.; Bader, M.; Williams, B. O.; Warman, M. L.; Robling, A. G. Reply to Lrp5 Regulation of Bone Mass and Gut Serotonin Synthesis. *Nat. Med.* **2014**, *20*, 1229−1230.
(33) Brown, S.; Spudich, J. Cytochalasin Inhibits the Rate of Elongation of Actin Filament Fragments. *J. Cell Biol.* **1979**, *83*, 657−662.
(34) Zhang, J.; Zhang, X.; Zhang, L.; Zhou, F.; van Dinther, M.; Ten Dijke, P. LRP8 Mediates Wnt/β-Catenin Signaling and Controls Osteoblast Differentiation. *J. Bone Miner. Res.* **2012**, *27*, 2065−2074.
(35) Hutson, H. N.; Marohl, T.; Anderson, M.; Eliceiri, K.; Campagnola, P.; Masters, K. S. Calcific Aortic Valve Disease Is Associated with Layer-Specific Alterations in Collagen Architecture. *PLoS One* **2016**, *11*, No. e0163858.
(36) Joll, J. E., 2nd; Clark, C. R.; Peters, C. S.; Raddatz, M. A.; Bersi, M. R.; Merryman, W. D. Genetic Ablation of Serotonin Receptor 2B Improves Aortic Valve Hemodynamics of Notch1 Heterozygous Mice in a High-Cholesterol Diet Model. *PLoS One* **2020**, *15*, No. e0238407.
(37) Fong, F.; Xian, J.; Demer, L. L.; Tintut, Y. Serotonin Receptor Type 2B Activation Augments TNF-α-Induced Matrix Mineralization in Murine Valvular Interstitial Cells. *J. Cell. Biochem.* **2021**, *122*, 249−258.
(38) Gu, X.; Masters, K. S. Role of the MAPK/ERK Pathway in Valvular Interstitial Cell Calcification. *Am. J. Physiol.: Heart Circ. Physiol.* **2009**, *296*, H1748−H1757.
(39) Monzack, E. L.; Masters, K. S. Can Valvular Interstitial Cells Become True Osteoblasts? A Side-by-Side Comparison. *J. Heart Valve Dis.* **2011**, *20*, 449−463.
(40) Hjortnaes, J.; Goettsch, C.; Hutcheson, J. D.; Camci-Unal, G.; Lax, L.; Scherer, K.; Body, S.; Schoen, F. J.; Kluin, J.; Khademhosseini, A.; Aikawa, E. Simulation of Early Calcific Aortic Valve Disease in a 3D Platform: A Role for Myofibroblast Differentiation. *J. Mol. Cell. Cardiol.* **2016**, *94*, 13−20.
(41) Yip, C. Y. Y.; Chen, J.-H.; Zhao, R.; Simmons, C. a. Calcification by Valve Interstitial Cells Is Regulated by the Stiffness of the Extracellular Matrix. *Arterioscler., Thromb., Vasc. Biol.* **2009**, *29*, 936−942.
(42) Richards, J.; El-Hamamsy, I.; Chen, S.; Sarang, Z.; Sarathchandra, P.; Yacoub, M. H.; Chester, A. H.; Butcher, J. T. Side-Specific Endothelial-Dependent Regulation of Aortic Valve Calcification: Interplay of Hemodynamics and Nitric Oxide Signaling. *Am. J. Pathol.* **2013**, *182*, 1922−1931.
(43) Quinlan, A. M. T.; Billiar, K. L. Investigating the Role of Substrate Stiffness in the Persistence of Valvular Interstitial Cell Activation. *J. Biomed. Mater. Res., Part A* **2012**, *100*, 2474−2482.
(44) Yang, C.; Tibbitt, M. W.; Basta, L.; Anseth, K. S. Mechanical Memory and Dosing Influence Stem Cell Fate. *Nat. Mater.* **2014**, *13*, 645−652.
(45) Wiltz, D. C.; Han, R. I.; Wilson, R. L.; Kumar, A.; Morrisett, J. D.; Grande-Allen, K. J. Differential Aortic and Mitral Valve Interstitial Cell Mineralization and the Induction of Mineralization by Lysophosphatidylcholine In Vitro. *Cardiovasc. Eng. Technol.* **2014**, *5*, 371−383.
(46) Lacerda, C. M. R.; MacLea, H. B.; Kisiday, J. D.; Orton, E. C. Static and Cyclic Tensile Strain Induce Myxomatous Effector Proteins and Serotonin in Canine Mitral Valves. *J. Vet. Cardiol.* **2012**, *14*, 223−230.
(47) Peacock, J. D.; Levay, A. K.; Gillaspie, D. B.; Tao, G.; Lincoln, J. Reduced Sox9 Function Promotes Heart Valve Calcification Phenotypes in Vivo. *Circ. Res.* **2010**, *106*, 712−719.
(48) Zeng, Y.; Sun, R.; Li, X.; Liu, M.; Chen, S.; Zhang, P. Pathophysiology of Valvular Heart Disease (Review). *Exp. Ther. Med.* **2016**, *11*, 1184−1188.
(49) Yadav, V. K.; Ryu, J.-H.; Suda, N.; Tanaka, K. F.; Gingrich, J. A.; Schütz, G.; Glorieux, F. H.; Chiang, C. Y.; Zajac, J. D.; Insogna, K. L.;

https://doi.org/10.1021/acsomega.1c01723
ACS Omega 2021, 6, 19494−19505

Mann, J. J.; Hen, R.; Ducy, P.; Karsenty, G. Lrp5 Controls Bone Formation by Inhibiting Serotonin Synthesis in the Duodenum. *Cell* **2008**, *135*, 825−837.
(50) Lacerda, C. M. R.; Orton, E. C. Evidence of a Role for Tensile Loading in the Pathogenesis of Mitral Valve Degeneration. *J. Clin. Exp. Cardiol.* **2012**, *3*, 2.
(51) Galli, C.; Macaluso, G.; Passeri, G. Serotonin: A Novel Bone Mass Controller May Have Implications for Alveolar Bone. *J. Negat. Results BioMed.* **2013**, *12*, 12.
(52) Kheradvar, A.; Zareian, R.; Kawauchi, S.; Goodwin, R. L.; R, S. Animal Models for Heart Valve Research and Development. *Drug Discovery Today: Dis. Models* **2017**, *24*, 55−62.
(53) Xin, L.; Yao, W.; Peng, Y.; Lu, P.; Ribeiro, R.; Wei, B.; Gellner, B.; Simmons, C.; Zu, J.; Sun, Y.; Badiwala, M. Primed Left Ventricle Heart Perfusion Creates Physiological Aortic Pressure in Porcine Hearts. *ASAIO J.* **2020**, *66*, 55−63.
(54) Zhong, A.; Mirzaei, Z.; Simmons, C. A. The Roles of Matrix Stiffness and SS-Catenin Signaling in Endothelial-To_Mesenchymal Transition of Aortic Valve Endothelial Cells. *Cardiovasc. Eng. Technol.* **2018**, *9*, 158−167.
(55) Cloyd, K. L.; El-Hamamsy, I.; Boonrungsiman, S.; Hedegaard, M.; Gentleman, E.; Sarathchandra, P.; Colazzo, F.; Gentleman, M. M.; Yacoub, M. H.; Chester, A. H.; Stevens, M. M. Characterization of Porcine Aortic Valvular Interstitial Cell "Calcified" Nodules. *PLoS One* **2012**, *7*, No. e48154.
(56) Wang, X.; Lee, J.; Ali, M.; Kim, J.; Lacerda, C. M. R. Phenotype Transformation of Aortic Valve Interstitial Cells Due to Applied Shear Stresses Within a Microfluidic Chip. *Ann. Biomed. Eng.* **2017**, *45*, 2269−2280.
(57) Hasan, A.; Ragaert, K.; Swieszkowski, W.; Selimović, S.; Paul, A.; Camci-Unal, G.; Mofrad, M. R. K.; Khademhosseini, A. Biomechanical Properties of Native and Tissue Engineered Heart Valve Constructs. *J. Biomech.* **2014**, *47*, 1949−1963.
(58) Ting-Beall, H. P.; Lee, A. S.; Hochmuth, R. M. Effect of Cytochalasin D on the Mechanical Properties and Morphology of Passive Human Neutrophils. *Ann. Biomed. Eng.* **1995**, *23*, 666−671.
(59) Gomori, G. A Raipd One-Step Trichrome Stain. *Am. J. Clin. Pathol.* **1950**, *20*, 661−664.

https://doi.org/10.1021/acsomega.1c01723
ACS Omega 2021, 6, 19494−19505